NASA TECHNICAL MEMORANDUM

NASA TM X-1323

GENERAL METHOD FOR PREDICTING EFFICIENCY OF PARABOLOIDAL SOLAR COLLECTOR

by Gabriel N. Kaykaty

Lewis Research Center

Cleveland, Ohio

NATIONAL AERONAUTICS AND SPACE ADMINISTRATION • WASHINGTON, D. C. • DECEMBER 1966

NASA TM X-1323

GENERAL METHOD FOR PREDICTING EFFICIENCY OF PARABOLOIDAL SOLAR COLLECTOR

By Gabriel N. Kaykaty

Lewis Research Center
Cleveland, Ohio

NATIONAL AERONAUTICS AND SPACE ADMINISTRATION

For sale by the Clearinghouse for Federal Scientific and Technical Information
Springfield, Virginia 22151 – Price $2.00

CONTENTS

GENERAL METHOD FOR PREDICTING EFFICIENCY OF PARABOLOIDAL SOLAR COLLECTOR

by Gabriel N. Kaykaty

Lewis Research Center

SUMMARY

A technique and working curves are presented for the rapid calculation of the maximum collection efficiency of a paraboloidal collector that focuses solar energy into a cavity receiver. Effects of collector surface errors, orientation error, and rim angle are included. Any distribution of surface errors may be specified in the method.

Results of a comparison between this technique and a rigorous analysis for a collector with a normal distribution of surface error demonstrate that the two methods of calculation predict essentially the same maximum collection efficiency in the absence of orientation error. When the system is misoriented, the maximum collection efficiency is 1 percentage point lower than the refined calculation for the range of misorientation up to 30 minutes at a receiver operating temperature of 2200° R and less than 1.5 percentage points lower at a receiver operating temperature of 4000° R.

The favorable agreement in the compared values of collection efficiencies indicates that the presented technique is sufficiently accurate for use in solar-power-systems analysis.

INTRODUCTION

Solar energy, which has been the major source of energy for Earth satellites and space probes up to the present, is being converted into electrical energy exclusively through the use of solar cells. In order to provide the electric power for future space missions, the use of solar energy is being considered with various other energy-conversion devices such as thermoelectric, turbodynamic, and thermionic converters. These devices operate at high temperature and require concentration of the relatively low intensity of radiation that exists in space. A solar collection system concentrates and absorbs solar radiation for delivery to the energy-conversion system.

The collection system considered herein consists of a paraboloidal collector with a cavity receiver. The paraboloid was selected since, theoretically, it is capable of the maximum concentration of solar radiation and, therefore, will provide the highest collection efficiency. A highly efficient collection system contributes to a reduction both in the total weight and in the size of the solar power system.

One expedient and simple method for predicting the collection system efficiency for a systems analysis is to base the performance calculations on a receiver aperture diameter that is sized to capture all the energy reflected from the collector. This conservative approach in sizing the aperture to collect energy of low density in the fringe of the reflected energy field imposes a penalty on the performance in the form of a higher radiation loss from the receiver.

The penalty increases with increasing temperature, orientation error, and surface error; this increase results in a significant departure from the effective utilization of available solar energy.

In order to attain a higher performance, it is advantageous to reduce the receiver aperture diameter, which diminishes the receiver radiation losses while simultaneously reducing the amount of energy entering the receiver. The aperture diameter can be decreased until the reduction of radiation losses balances the reduction in solar energy entering the receiver.

To determine this point at which maximum performance occurs requires a knowledge of the energy distribution in the plane of the receiver aperture. This energy distribution is a function of the surface and orientation accuracy and the rim angle of the collector. Because the Sun is not a point source, the radiation reflected from any single point of the collector surface is spread over an area of the focal plane and is not concentrated at the focus. Since this spread of energy affects the power distribution, the concept of cone tracing rather than ray tracing must be applied.

Some investigators (ref. 1) employ cone optics in an attempt to predict the effect of collector inaccuracies on the concentration of solar radiation. They utilize a concept of a scattering circle, which applies some degree of statistics to the scatter of energy in the focal plane; however the resulting distribution is not related to the actual inaccuracies in the collector. Another statistical approach is employed in reference 2, in which a normal distribution of energy in the focal plane is assumed, but again no relation is established between the distribution of energy in the focal plane and the condition of the collector surface.

A more suitable approach is the association of the energy distribution in the focal plane with the surface errors in the actual collector; statistics can be applied, when necessary, to these errors. This approach is attempted in reference 3, but several simplifying assumptions are used to attain a mathematical solution. Only a normal

distribution of errors in the surface of the collector is included in the analysis, while the effect of misorientation is not considered.

A comprehensive analysis employing cone optics is undertaken in reference 4 to determine the energy distribution in the focal plane as a function of surface and orientation error. Statistics are applied to the reflection of energy from the collector surface. This method is free of simplifying assumptions and provides accurate results, but it requires a considerable amount of computer time to perform the calculations.

The analysis developed herein determines the distribution of energy in the focal plane using cone optics, so that the effects of the subtended angle of the Sun are included, and considers the effect of collector surface error, orientation error, and rim angle. Surface errors are described by the specification of the angular deviation of the surface normal to the actual surface from the normal to the ideal surface. The total magnitude of this angular deviation is assumed to exist in the plane of the optic axis.

For dealing with the effects of misorientation, this analysis employs a simplifying approximation that reduces appreciably the computational effort involved and results in only a slightly larger spread of energy over the focal plane. Using the results of the analysis, the fraction of total available energy captured by the receiver as a function of various aperture sizes is calculated for numerous combinations of surface errors, orientation errors, and paraboloidal rim angles. This information is presented in the form of working curves, which in combination with the receiver operating temperature and cavity conditions are sufficient to calculate the efficiency of the collection system for any application. A convenient method is presented of employing the working curves to predict the efficiency of a paraboloidal collection system, for which the concentrator may have any specified distribution of surface error. An example is provided to demonstrate the technique.

METHOD OF ANALYSIS

The following assumptions are incorporated in the analysis:

(1) The Sun radiates with uniform intensity over its surface.

(2) The energy is uniform over the elliptical image formed on the focal plane by reflection from any single point on the surface of the concentrator.

(3) Each error is spread uniformly over the surface of the concentrator when a distribution of errors is present.

(4) The surface error in the concentrator is assumed only in the plane of the optic axis.

From the standpoint of engineering calculations, the approximations introduced by assumptions (1) and (3) have a negligible effect on the results of this analysis.

PARABOLIC COLLECTION SYSTEM

A schematic diagram of a parabolic collection system is presented in figure 1. It consists of a paraboloidal reflector and a cavity receiver. The line passing through the

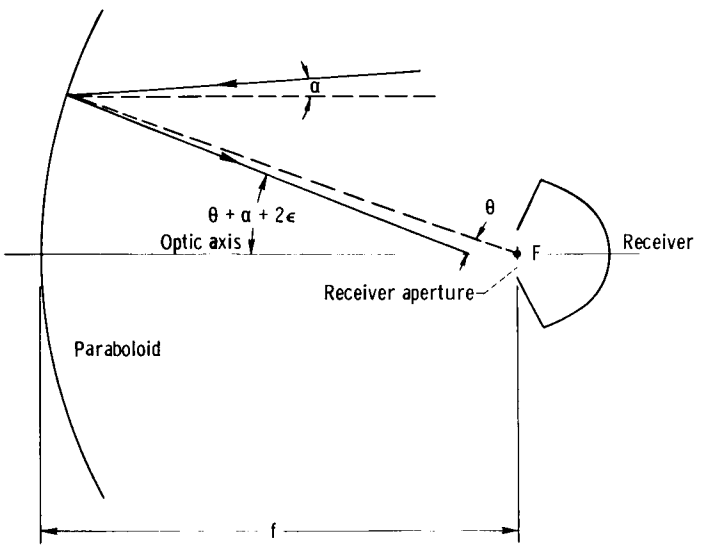

Figure 1. - Schematic of solar collection system.

center of the paraboloid and the center of the receiver forms the optic axis. The angle between the optic axis and the line joining the center of the collector with the center of the solar disk is the misorientation angle. The focal length f measures the distance between the center of the paraboloid and the focus of the paraboloid along the optic axis. All rays incident to the collector and parallel to the optic axis will, on reflection from a perfect collector surface, pass through the focus. The receiver aperture is in the focal plane centered at the focus. The ray reflected from the center of the paraboloid and originating from the center of the solar disk forms the geometric center of the image in the focal plane. The equation of the parabola in polar coordinates with the origin at the focus is

$$\rho = \frac{2f}{1 + \cos \theta} \tag{1}$$

where θ measures the angular position of any point of the collector. (All symbols are defined in appendix A.)

Concentration by Perfect Paraboloid

A cone of light reflected from any point on the surface of a paraboloid forms an

ellipse on the focal plane. The center of the ellipse is located at the focus when the incident cone of radiation is reflected from any point of a perfect paraboloid. The semiminor axis of the ellipse on the focal plane is defined as

$$b = \rho \tan \alpha \tag{2}$$

and the semimajor axis is defined by

$$a = \frac{\rho \tan \alpha}{\cos \theta} \tag{3}$$

where α is the half-angle subtended by the Sun at the collector, that is, the semicone angle of the incident radiation.

The area of the ellipse increases as θ increases; the energy reflected from the paraboloid is therefore distributed over a larger region of the focal plane.

A circular segment of the paraboloidal collector $d\theta$ with its average value at the location θ is shown in figure 2. The axis of the ellipse projected from this segment

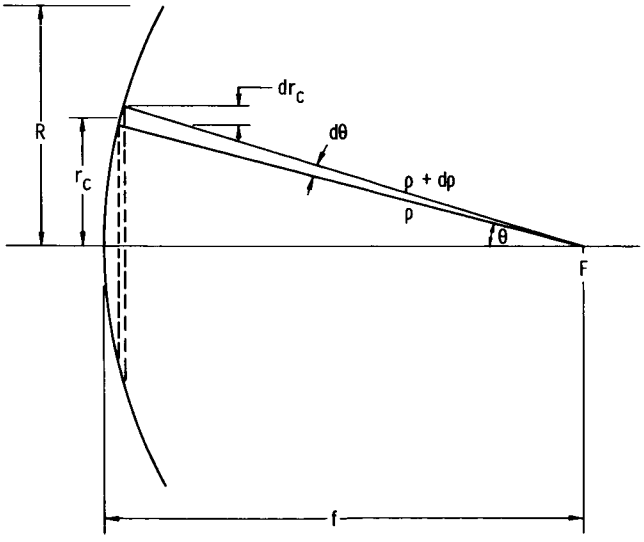

Figure 2. - Collector geometric parameters.

rotates in the focal plane as solar energy is reflected from various positions around this element of the paraboloid. All the ellipses are distributed uniformly around the focus, which is the center of the image, and the energy delivered to any radius r about the focus is symmetric. For the perfect paraboloid, the centers of all ellipses reflected from the collector coincide at the focus, as in figure 3(a), to produce the maximum concentration of energy.

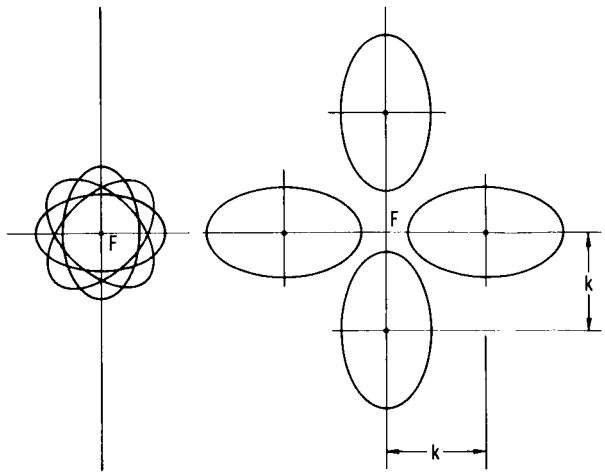

(a) Maximum concentration of energy. (b) Distribution of energy with concentrator surface error.

Figure 3. - Energy patterns in focal plane of collector.

Effect of Collector Surface Accuracy

In order to depict reasonably the physical properties of the collector as associated with its surface accuracy, a practical error model is constructed, which describes the imperfections in the concentrator surface by a deviation of the normal to the ideal paraboloidal surface. This deviation ϵ is assumed to lie in the plane of the optic axis.

An imperfect collector will scatter the reflected energy over the focal plane by displacing the centers of the ellipses radially from the focus and thereby reduce the concentration of collected energy. Thus, when an incident cone of light is reflected from a point on the collector with an angular surface error ϵ, it will intercept the focal plane as an ellipse with its center displaced a distance $k = \frac{\rho \tan 2\epsilon}{\cos \theta}$ from the focus. The distance an ellipse is displaced increases with increasing value of θ.

With a given surface error, the ellipses are equally displaced from the focus for any circular element $d\theta$. Consequently, the centers of the ellipses are located uniformly in a circle about the focus, as shown in figure 3(b), with a radius $k = \frac{\rho \tan 2\epsilon}{\cos \theta}$. The energy is therefore distributed symmetrically for any radial position about the focus.

The total energy associated with any ellipse reflected from a position θ on the collector is the energy intercepted by the collector segment $d\theta$ with the average value of θ. The quantity of energy E_θ is given by the following expression which is derived in appendix B:

$$E_\theta = 2\pi K \rho^2 \sin \theta \, d\theta \tag{4}$$

DETERMINATION OF ENERGY DISTRIBUTION IN FOCAL PLANE

Perfectly Oriented Paraboloidal Collector

In order to determine the energy distribution in the focal plane, the contribution of

energy from each ring element of the paraboloid collector to the various circular regions around the focal plane is calculated. This is accomplished by locating in the focal plane the image of the Sun projected from every point of the collector as a function of the effective surface error. The energy associated with this image is then divided among the various zones of the focal plane that receive this radiation. The energy distribution is derived as a function of one error. The distribution of energy resulting from concentration by a collector with a distribution of errors is obtained by superimposing the energy profiles associated with each error.

A circular element dr is assumed in the focal plane with the average radius r centered about the focus F, as shown in figure 4. Any radius r will intercept the ellipse at the value of x given by

$$x = \frac{-ak \pm \sqrt{\left(a^2 - b^2\right)\left(r^2 - b^2\right) + b^2k^2}}{\left(a - \frac{b^2}{a}\right)} \tag{5}$$

The area of the element dr common to the ellipse is $2\varphi_t r\, dr$ where

$$\varphi_T = \varphi_1 + \varphi_2 \tag{6}$$

and

$$\varphi_1 = \cos^{-1}\left(\frac{k + x_1}{r}\right) \tag{7}$$

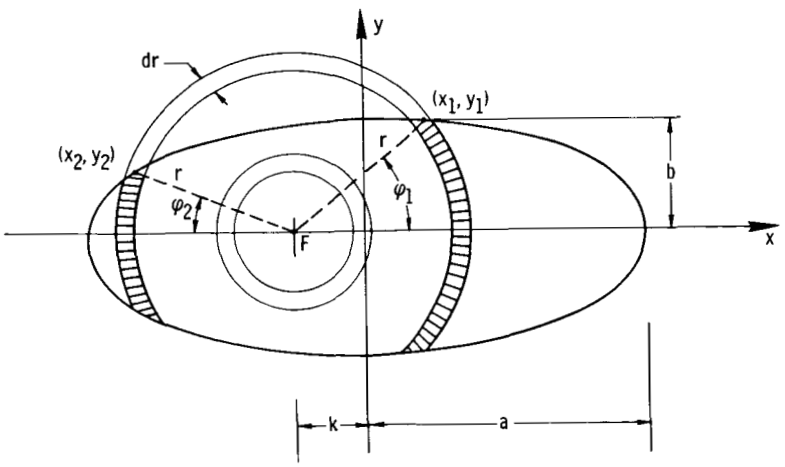

Figure 4. - Allocations of energy reflected from point of collector to various locations in focal plane.

$$\varphi_2 = \cos^{-1} - \left(\frac{k + x_2}{r}\right) \tag{8}$$

The quantity of energy allocated to the element dr is the fraction $(2\varphi_t r\ dr)/\pi ab$ of the energy associated with the ellipse, where this fraction is the ratio of the area of the element intercepting the ellipse to the area of the ellipse in the focal plane.

Since $2\pi K\rho^2 \sin\theta\ d\theta$ is the total energy delivered by a circular segment of the collector $d\theta$ to the entire ellipse, the energy assigned to the ring r dr is

$$dE = \frac{2\varphi_t}{\pi ab}\ r\ dr\ 2\pi K\rho^2 \sin\theta\ d\theta \tag{9}$$

The total energy E_{ce} deposited in the element dr is the sum of the contributions of energy from every segment of the collector and

$$E_{ce} = \int_{\theta=\theta_1}^{\theta=\theta_2} \frac{2\varphi_t\ r\ dr}{\pi ab}\ 2\pi K\rho^2 \sin\theta\ d\theta \tag{10}$$

The limits of integration θ_1 to θ_2 represent the section of the collector that contributes energy to any element dr and is a function of the position r.

The total energy in a circular region of the focal plane about the focus is the sum of the energy in all the elements dr in that region. Therefore,

$$E_T = \int_{r=r_1}^{r=r_2} 2Kr\ dr \int_{\theta=\theta_1}^{\theta=\theta_2} \frac{2\varphi_t}{ab}\ \rho^2 \sin\theta\ d\theta \tag{12}$$

If a receiver is positioned so that the center of its aperture is coincident with the focus, then the amount of energy entering the receiver is determined by equation (12), with the limits of integration on r from 0 to r_1, where r_1 is the radius of the receiver aperture.

The value of φ_t is a function of ϵ, θ, and r, and the limits of integration of θ are functions of ϵ and r. Since there is no analytical solution readily available for equation (12), the integration is performed by the numerical technique of substituting $\Delta\theta$ for $d\theta$ and Δr for dr.

Misoriented Paraboloidal Collector

Misorientation of the collection system, which displaces the optic axis from the Earth-Sun axis by the angular quantity β, will, in addition to collector surface error, scatter the reflected energy from the center of the image on the focal plane. The extent of this scattering varies with the circumferential position of the point on the surface of a ring element of the collector $d\theta$ from which energy is reflected. This variation will produce a nonsymmetrical distribution of energy about the center of the image. The center of the image is at a distance of $f \tan \beta$ from the focus, as illustrated in figure 5.

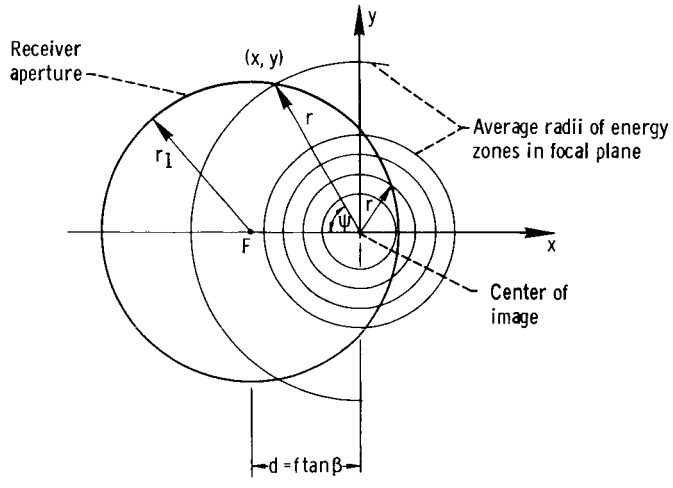

Figure 5. - Zones of focal plane delivering energy into receiver when collector is misoriented.

With any ring element of the collector, the ellipse reflected from the position that is in the plane of misorientation is displaced the largest distance from the center of the image and the focus. The center of this ellipse will be located at a distance of $[\rho \tan (2\epsilon + \beta)]/\cos \theta$ from the focus.

To simplify the analysis, it is assumed that all the ellipses reflected from a ring element of the collector $d\theta$ are scattered equally from the center of the image with the magnitude of the largest displacement; this assumption results in symmetry of the energy distribution in the focal plane.

The effect of this simplification is that energy from other positions around the element $d\theta$ is diffused over a slightly larger region of the focal plane. Thus, the total energy captured by a given receiver aperture will be smaller than actual, and the corresponding computation of the collection efficiency will result in a conservative value.

The distance between the center of the ellipse and the center of the image is given by

$$k = \frac{\rho \tan (2\epsilon + \beta)}{\cos \theta} - f \tan \beta \tag{13}$$

It should be noted that the distance an ellipse is displaced because of misorientation increases with increasing value of θ.

The allocation of energy to the various circular elements dr, surrounding the center of the image in the focal plane under the conditions of misorientation, will be similar to the procedure outlined herein for the oriented case, and the relation defined by equation (13) is substituted for k. Equation (10) is utilized to determine the energy in the various circular zones of the focal plane, which surround the center of the image at the distance of $f \tan \beta$ from the focus.

If the receiver is positioned with the center of its aperture coincident with the focus, the amount of energy entering the receiver is the sum of the quantities of energy in the various zones of the focal plane that are common to the receiver aperture. As illustrated in figure 5, the portion of energy in each zone E_F that enters the receiver is given by

$$E_F = \frac{\psi}{\pi} E_{ce} \tag{14}$$

where ψ/π is the fraction of the zone dr with average radius r that is common to the receiver aperture, and E_{ce} is the energy in that zone as calculated by equation (10).

It can also be observed from figure 5 that

$$\cos \psi = - \left(\frac{x}{r}\right)$$

or

$$\psi = \text{arc cos} - \frac{x}{r} \tag{15}$$

When $r < r_1 - f \tan \beta$, the value of ψ is π. Also,

$$x = \frac{r_1^2 - r^2}{2d} - \frac{d}{2} \tag{16}$$

The total energy entering the receiver is the sum of the energy in all zones common to the receiver aperture:

$$E_T = \int_{r=0}^{r=r_1+f\tan\beta} \frac{\Psi}{\pi} E_{ce} = \int_{r=0}^{r=r_1+f\tan\beta} \frac{\Psi}{\pi} 2Kr\, dr \int_{\theta=\theta_1}^{\theta=\theta_2} \frac{2\varphi_t}{ab} \rho^2 \sin\theta\, d\theta \qquad (17)$$

The integration of this expression can be performed by numerical techniques.

WORKING CURVES AND THEIR APPLICATION

The fraction of available energy entering the receiver η_E was calculated for various aperture diameters as a function of collector surface errors of 0 to 30 minutes in combination with misorientation errors of 0 to 30 minutes for paraboloidal rim angles from 45^o to 60^o. The results are presented in figure 6 as a function of the ratio of receiver to collector radius r_1/R.

The curves indicate that, as the collector surface and orientation error increase, the energy reflected from the collector diffuses over a larger area of the focal plane; thus, the concentration is reduced, and larger aperture sizes are required to capture any quantity of energy.

Increasing the rim angle of the collector increases the concentration of energy toward the center of the image while, at the same time, increasing slightly the spread of energy in the focal plane, as shown in figure 7. The effect is that small receiver aperture diameters will capture more energy with higher rim angle collectors. As the receiver aperture diameter increases, the reverse effect is prevalent.

It can be expected that an actual collector will have a surface containing some distribution of errors. When the distribution of these errors in terms of their probability is known, which designates the percentage of the collector area having the given error value, it is possible to construct the curve of energy entering a receiver of various aperture diameters from the information presented in working curves.

As plotted, the included curves are based on an assigned probability of 1 to any surface error. When a distribution of surface errors is present in the collector, the magnitude of the energy profile associated with any error value will be reduced in proportion to its probability.

The total energy entering through any receiver aperture is then the sum of the energy entering the receiver, which corresponds to each of the errors associated with the specified distribution.

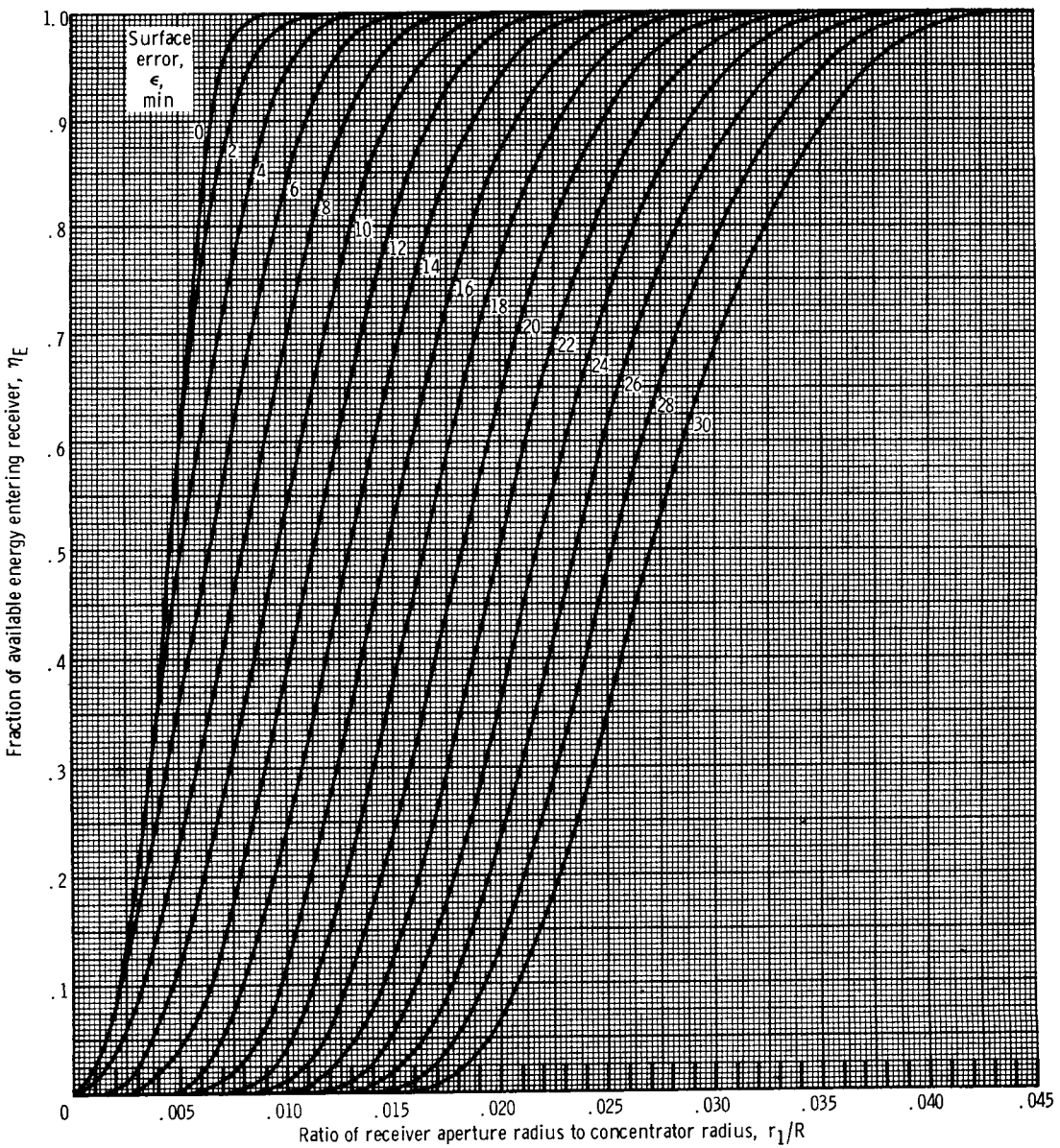

(a) Misorientation, 0 minutes; rim angle, 45°.

Figure 6. - Energy captured by receiver.

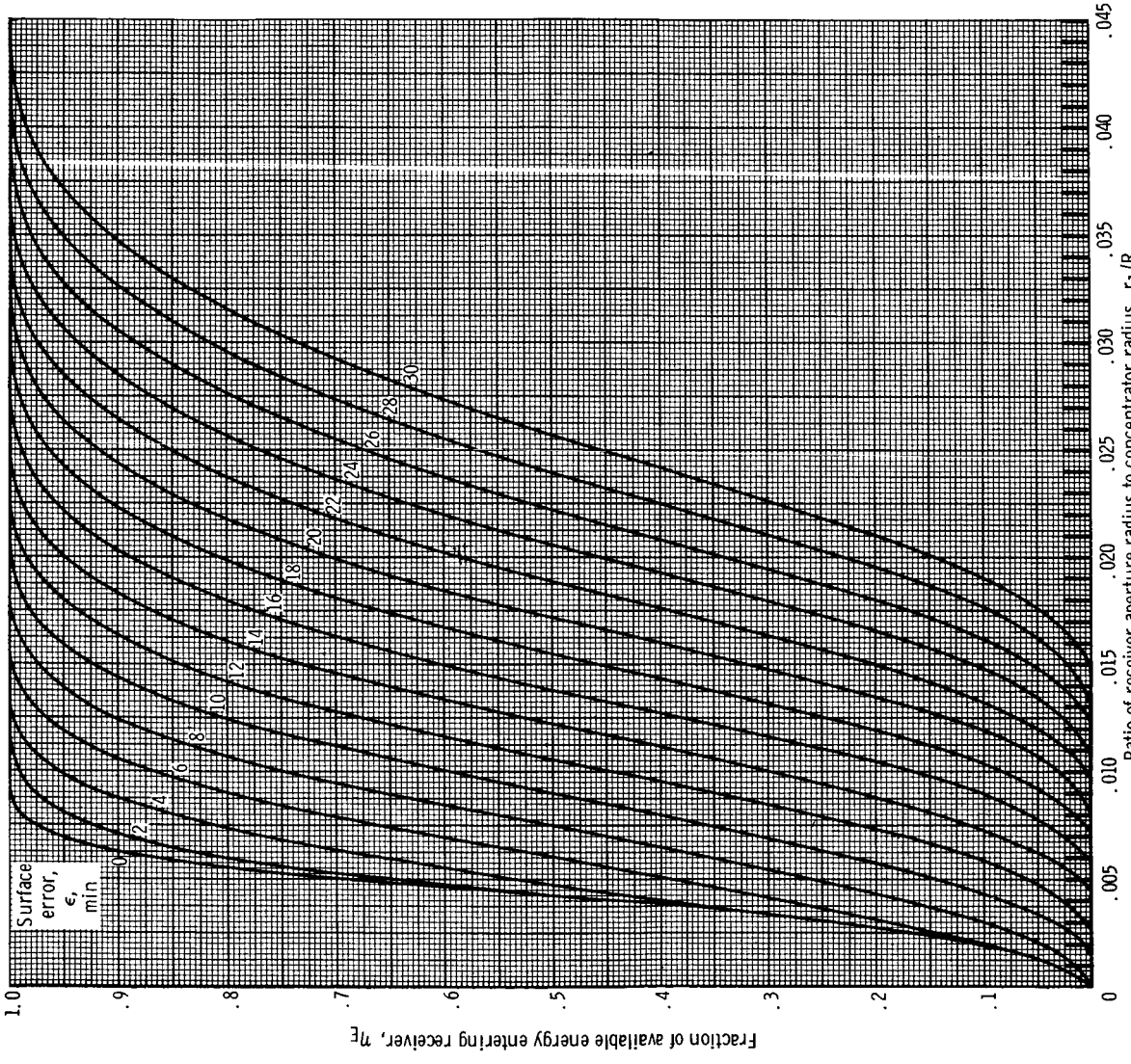

(b) Misorientation, 0 minutes; rim angle, 50°.

Figure 6. - Continued.

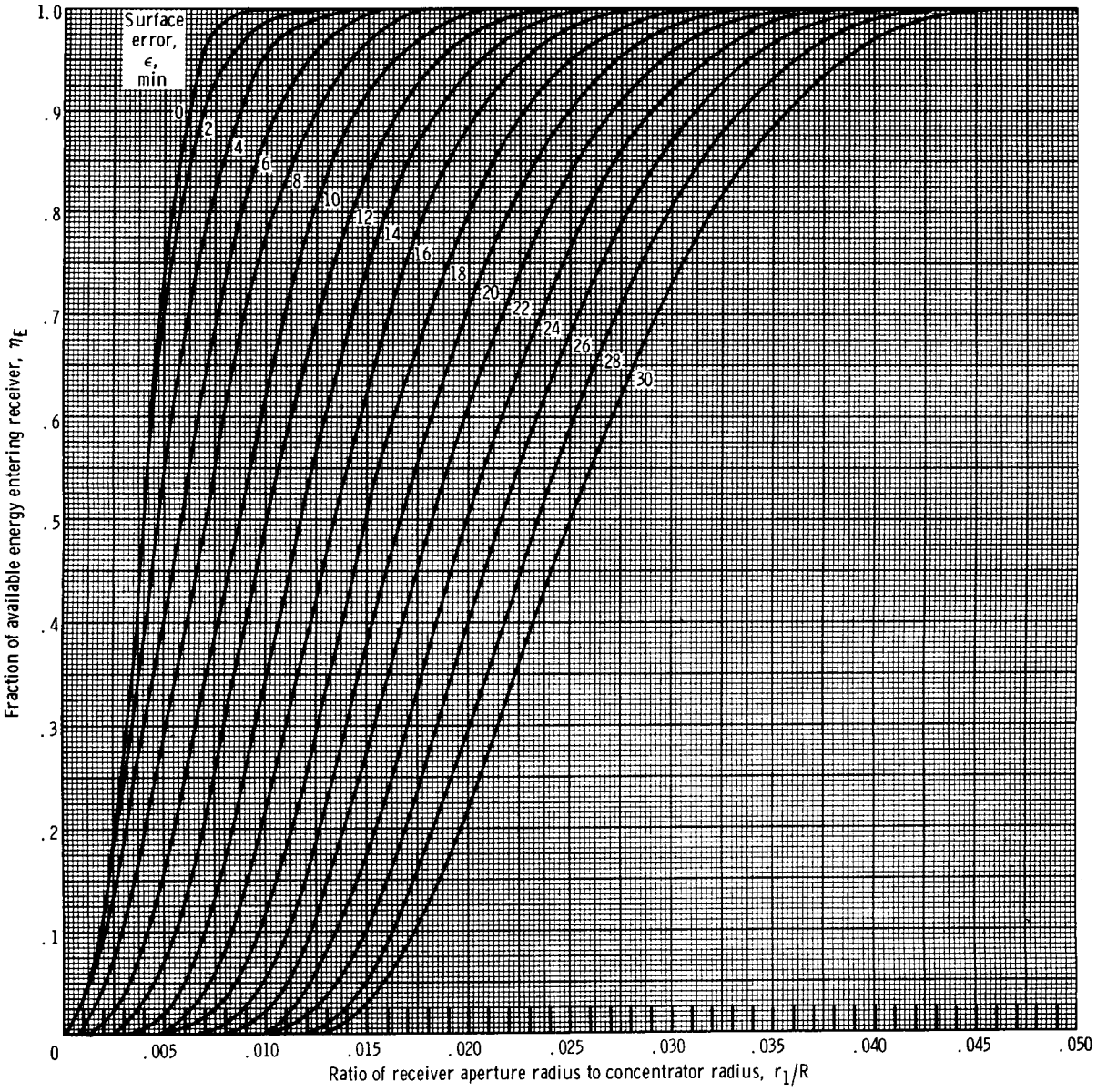

(c) Misorientation, 0 minutes; rim angle, 55°.

Figure 6. - Continued.

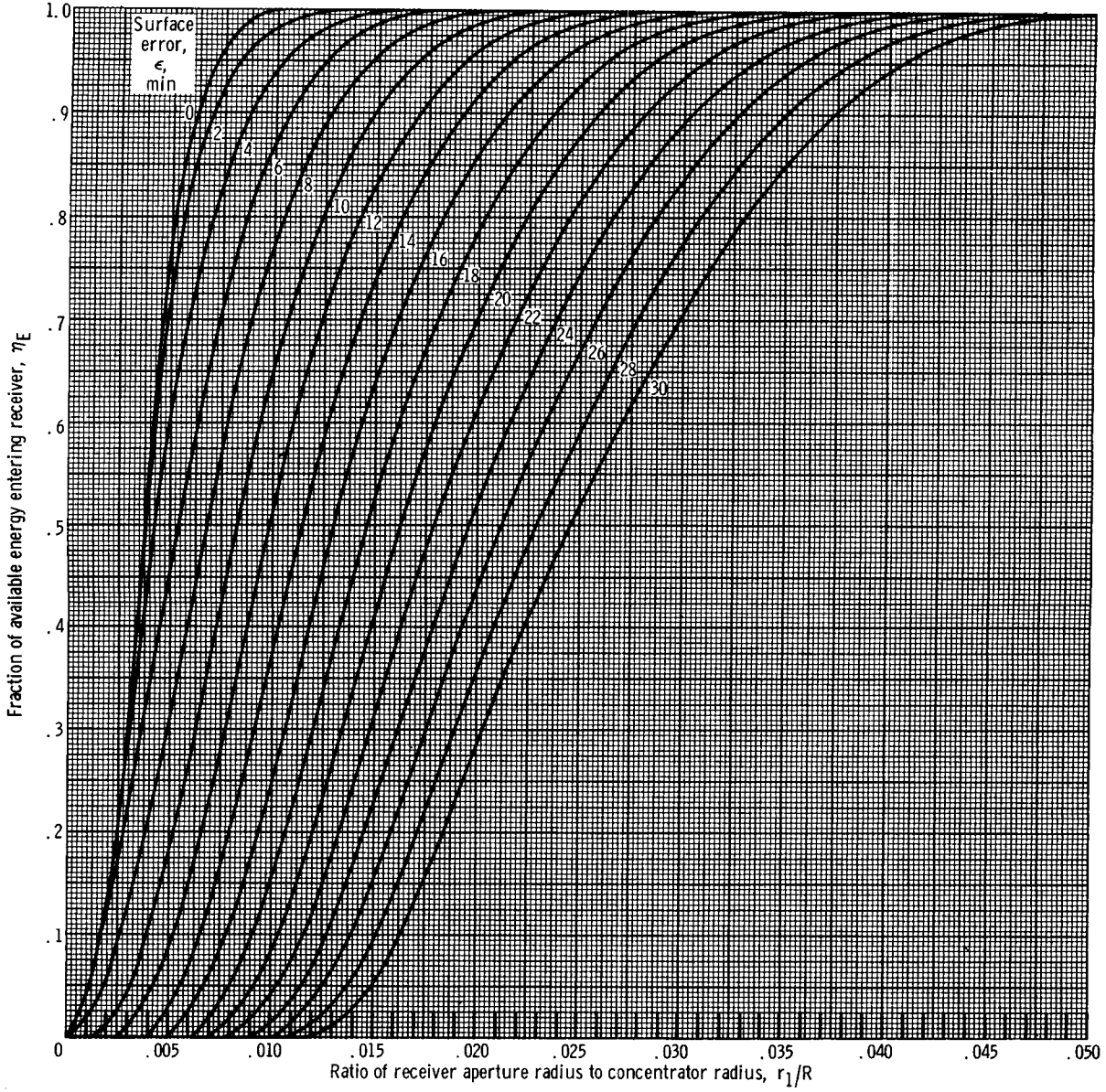

(d) Misorientation, 0 minutes; rim angle, 60°.

Figure 6. - Continued.

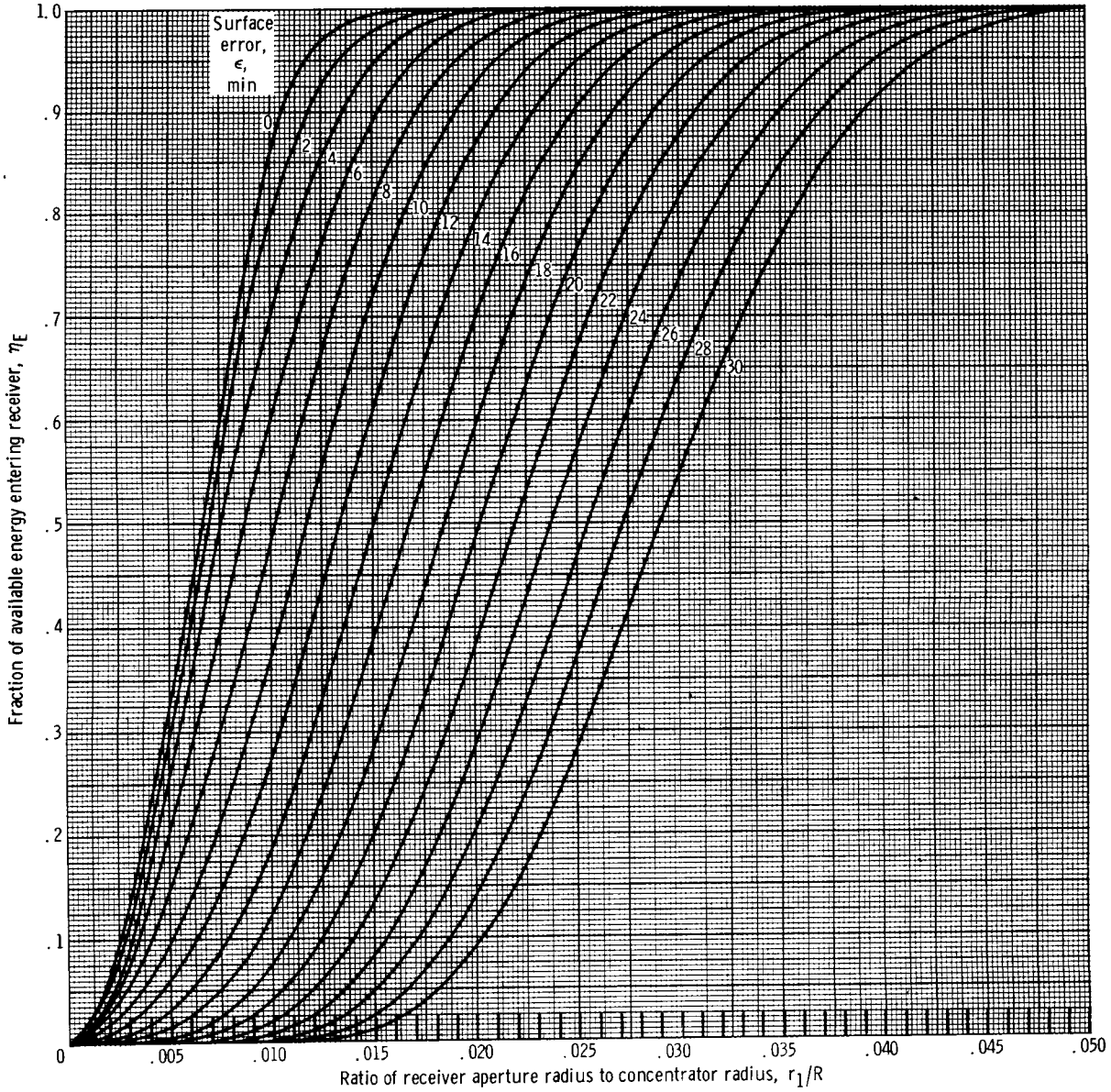

(e) Misorientation, 15 minutes; rim angle, 45°.

Figure 6. - Continued.

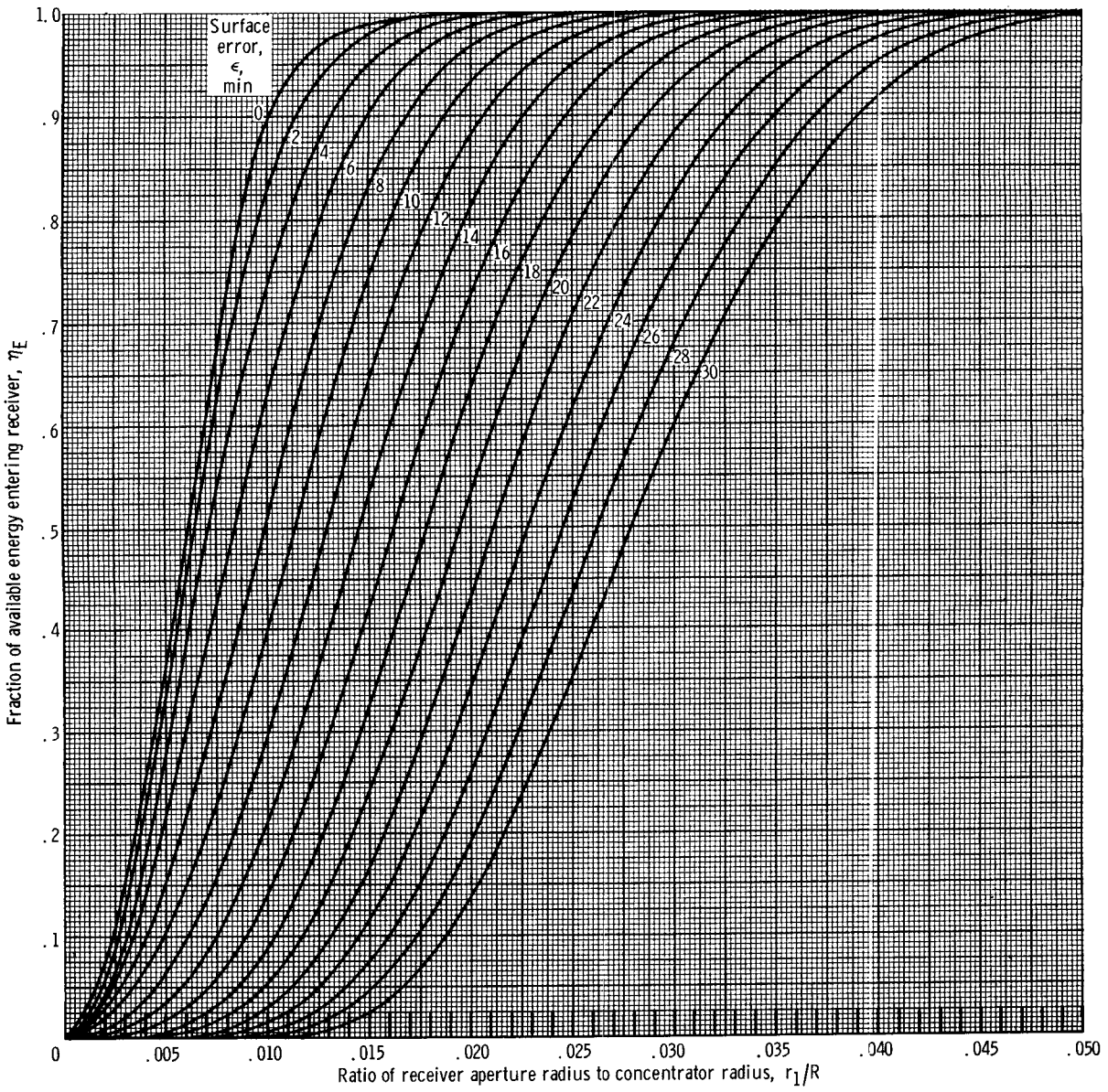

(f) Misorientation, 15 minutes; rim angle, 50°.

Figure 6. - Continued.

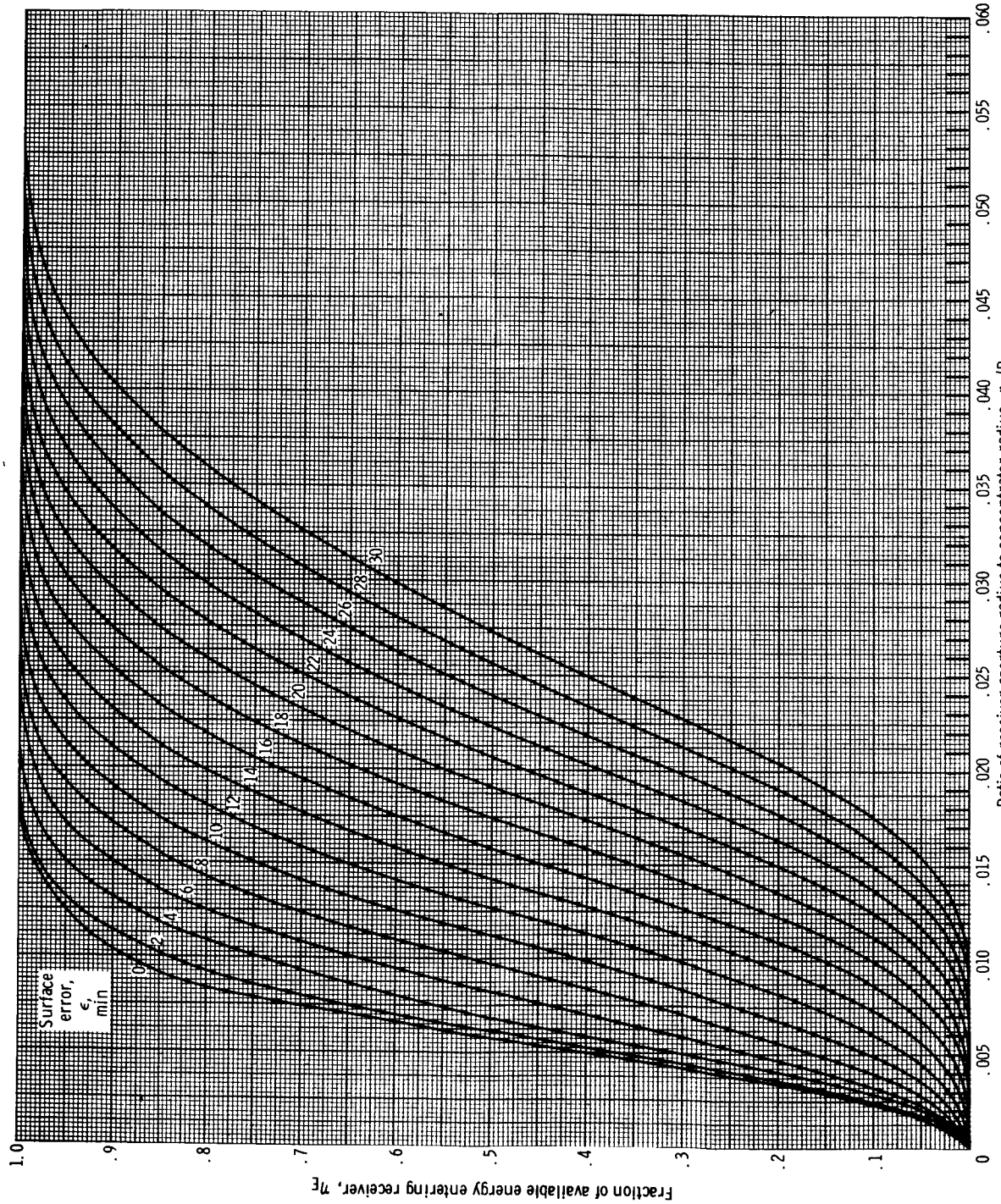

(g) Misorientation, 15 minutes; rim angle, 55°.

Figure 6. - Continued.

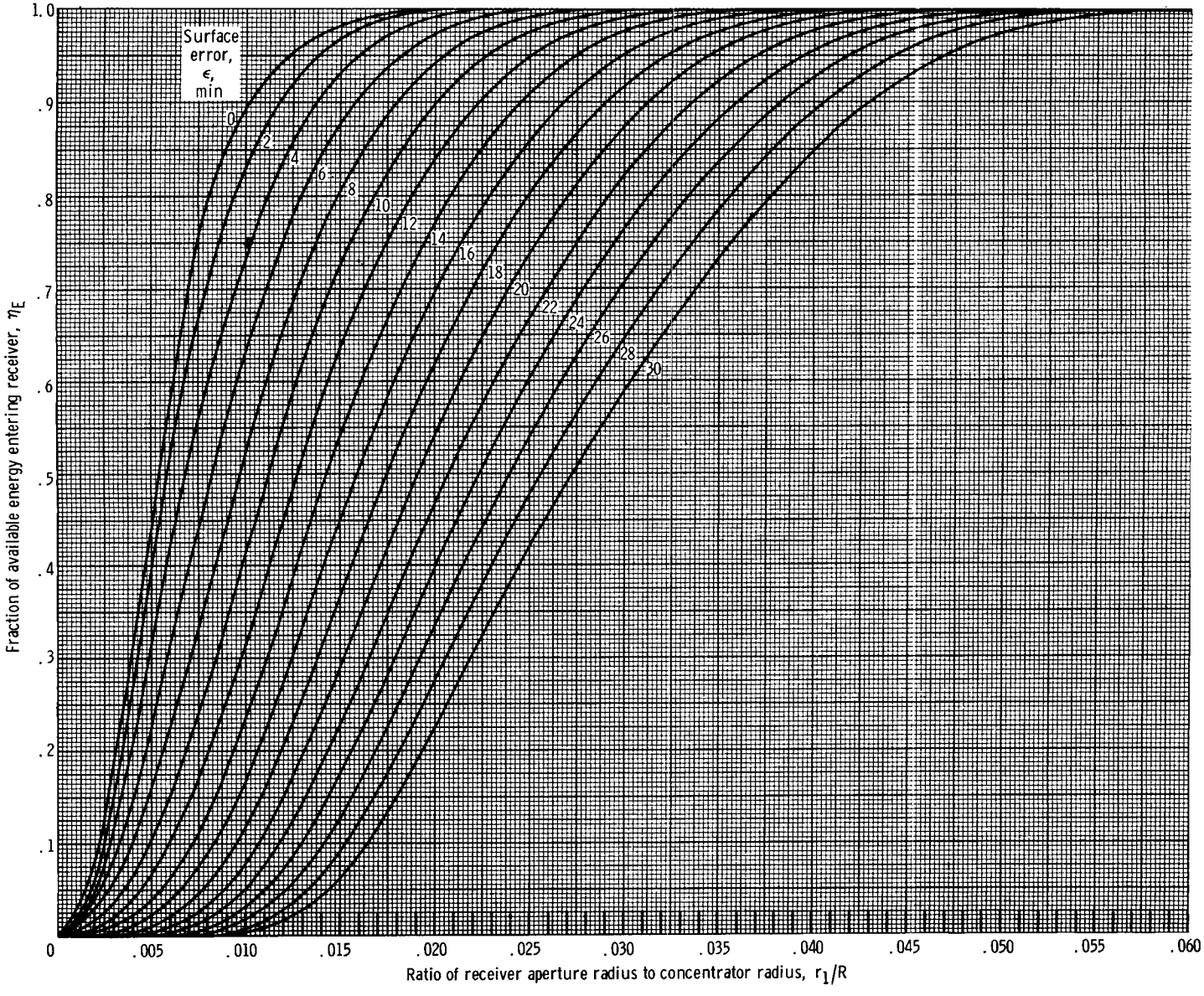

(h) Misorientation, 15 minutes; rim angle, 60°.

Figure 6. - Continued.

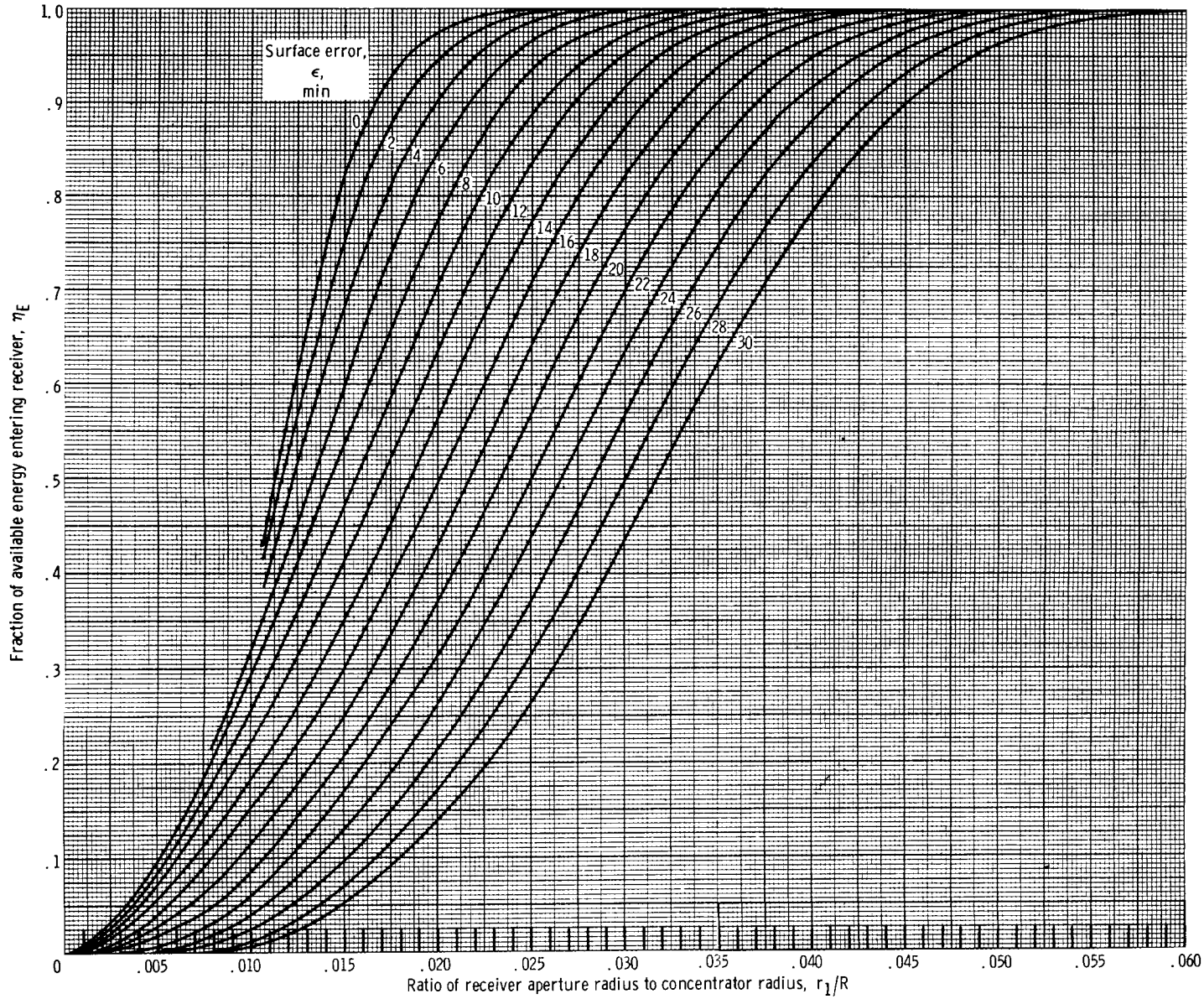

(i) Misorientation, 30 minutes; rim angle, 45°.

Figure 6. - Concluded.

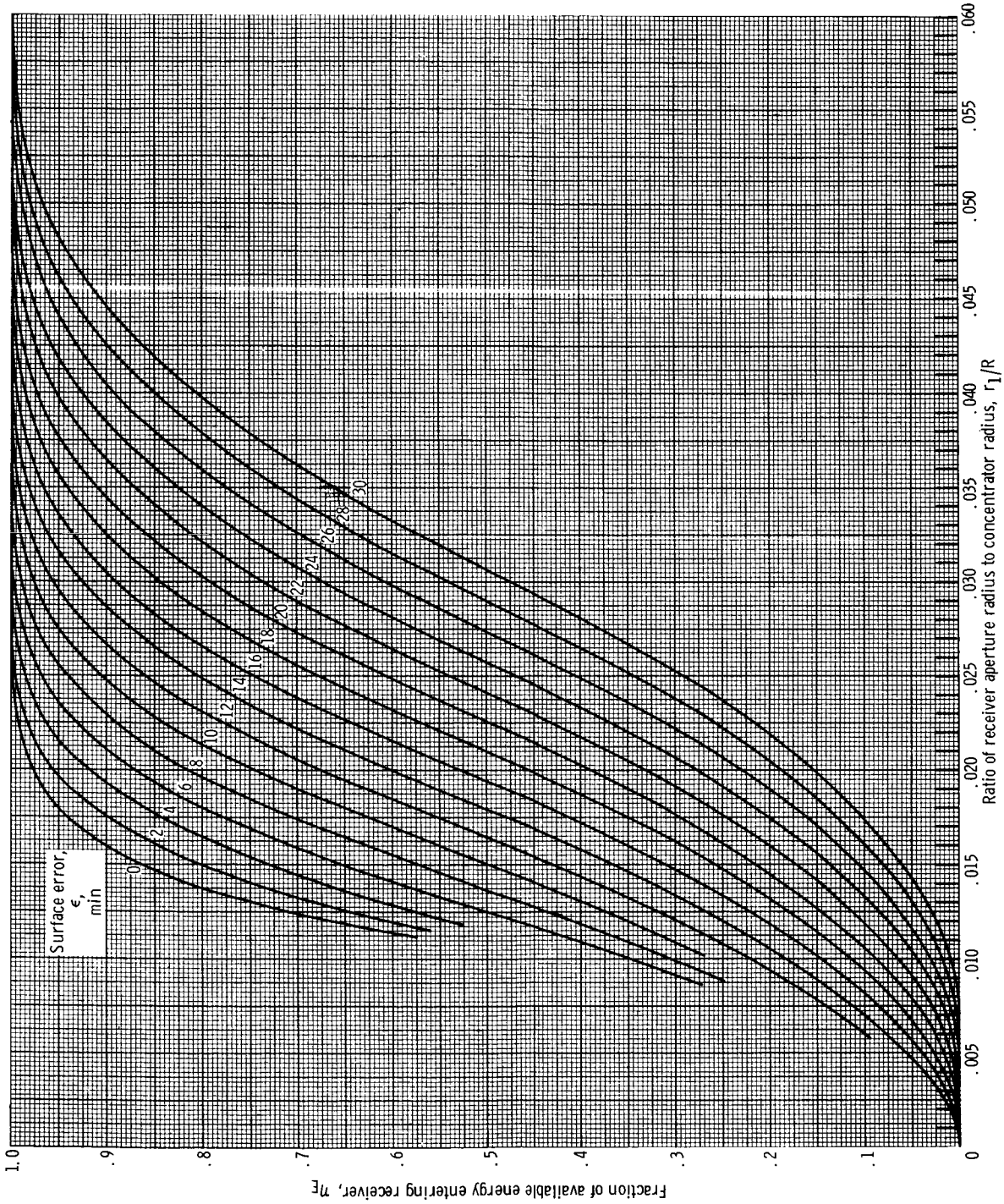

(j) Misorientation, 30 minutes; rim angle, 50°.

Figure 6. - Continued.

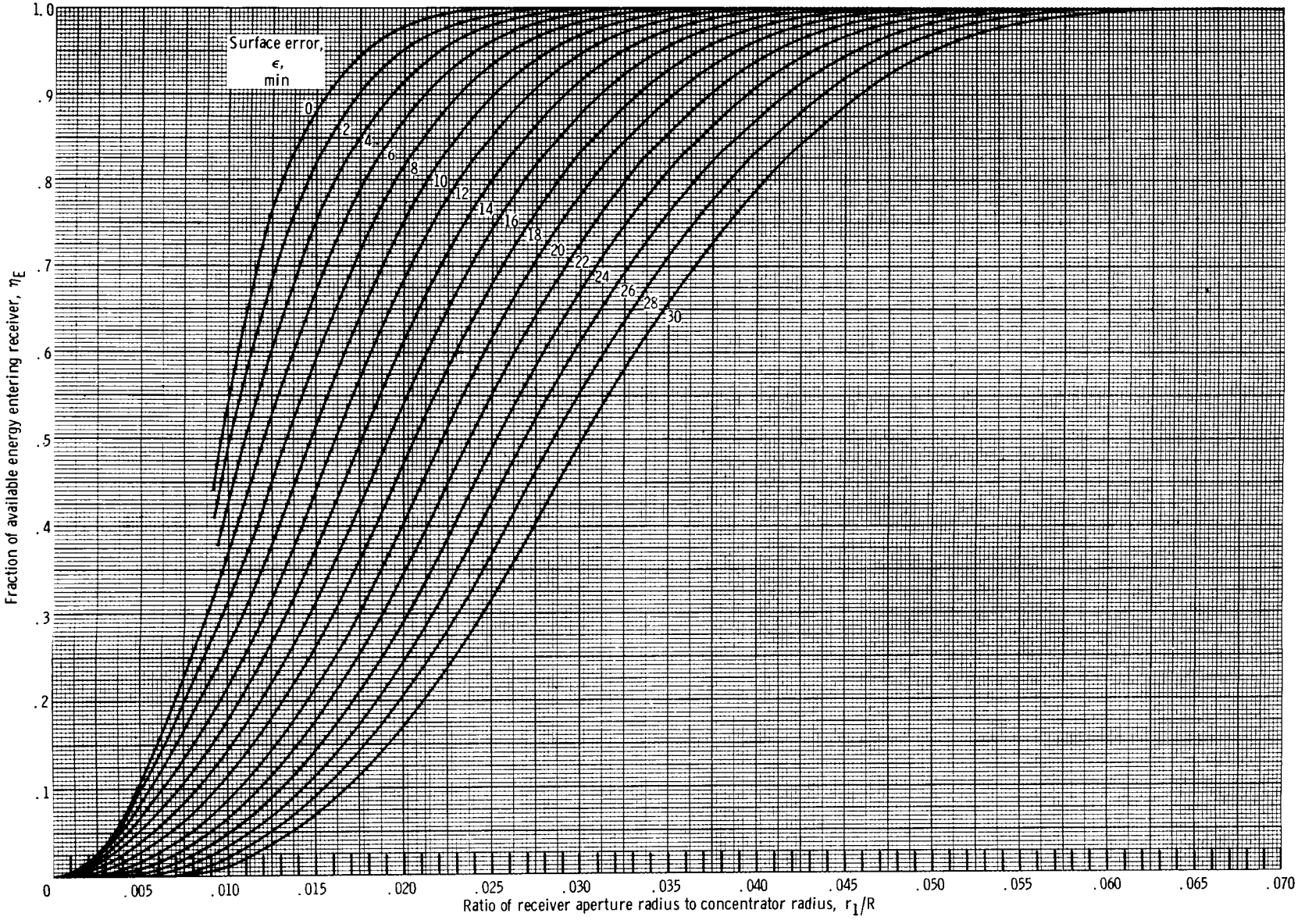

(k) Misorientation, 30 minutes; rim angle, 55°.

Figure 6. - Concluded.

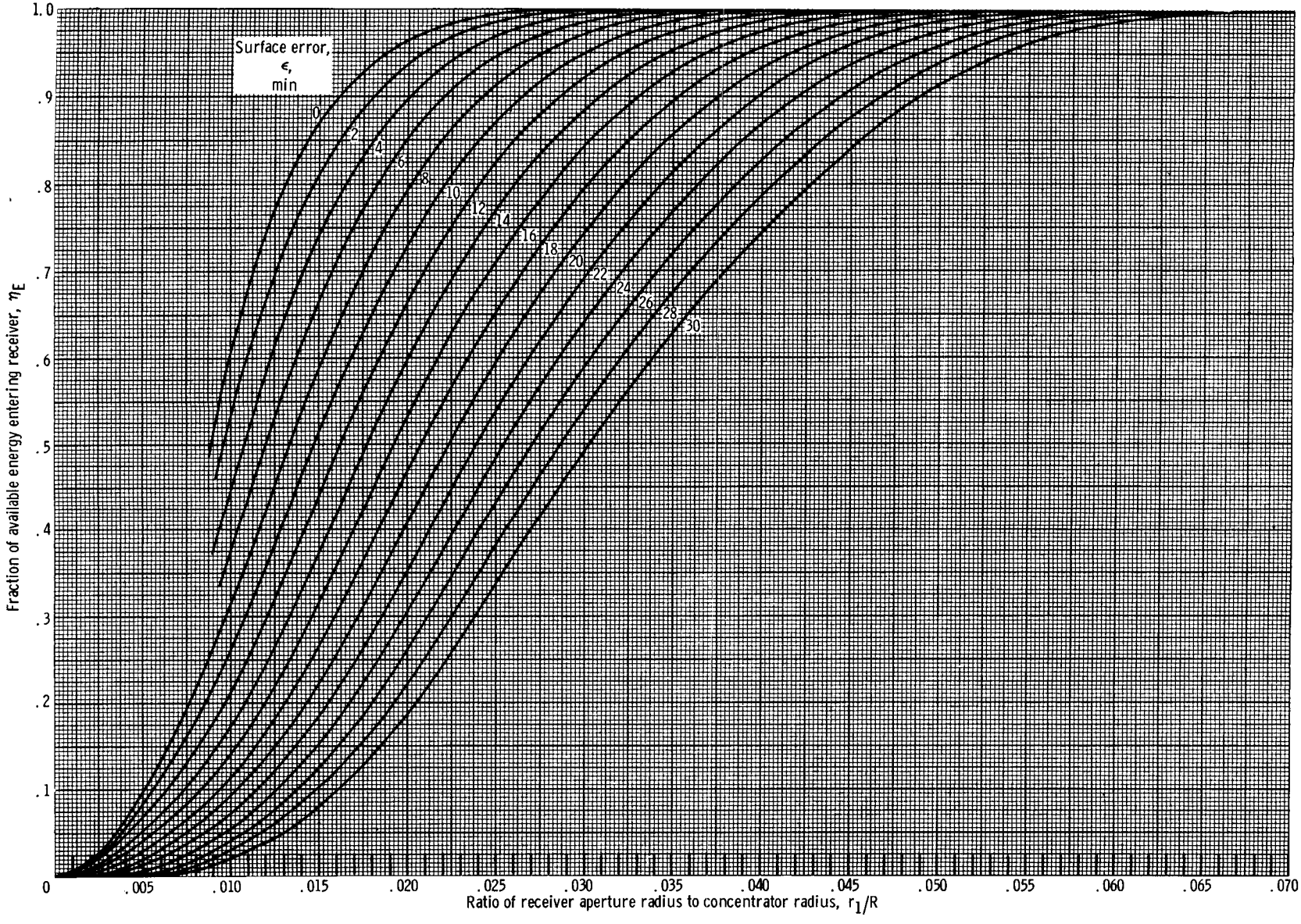

(*l*) Misorientation, 30 minutes; rim angle, 60°.

Figure 6. - Concluded.

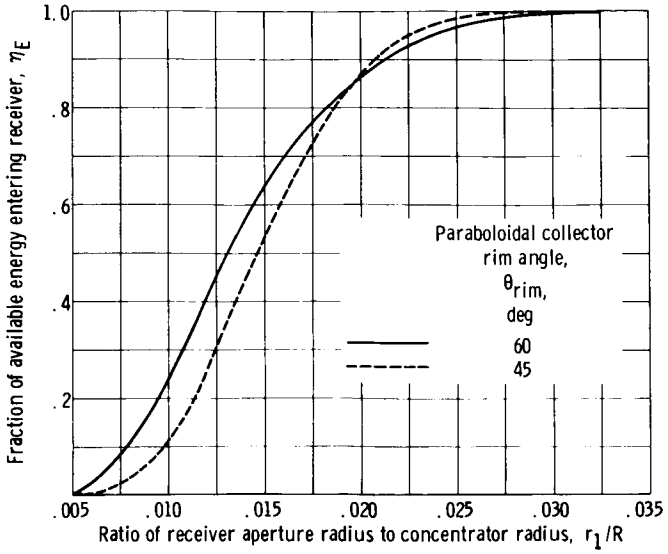

Figure 7. - Effect of rim angle on energy captured by receiver. Collector surface error, 16 minutes; collection system misorientation, 15 minutes.

The collection efficiency of a power system is determined according to

$$\eta_{c-a} = \eta_B \eta_R \eta_E \alpha_S - \frac{H\sigma A_{ra} T^4}{\pi R^2 K} \frac{\theta_o}{\theta_S} \tag{18}$$

where

$$\eta_B \eta_R \eta_E \alpha_S = \eta_c$$

and

$$\frac{H\sigma A_{ra} T^4}{\pi R^2 K} \frac{\theta_o}{\theta_S} = \eta_{rad}$$

Then,

$$\eta_{c-a} = \eta_c - \eta_{rad}$$

The collection efficiency η_{c-a} provides a measure of the net energy retained by the receiver for utilization by an energy conversion system after obstruction, reflection, and radiation losses have been considered and is expressed as the ratio of the net useful energy to the incident energy.

The concentration efficiency η_c increases with increasing receiver aperture area A_{ra} by virtue of the increasing value of η_E, while the radiation loss η_{rad} also increases. The maximum collection efficiency will be derived through a tradeoff between

these two quanities as the receiver aperture radius is varied. The procedure of applying the computed information to predict the collection efficiency of a power system is demonstrated in a sample calculation in appendix C.

TECHNIQUE EVALUATION

The performance of a paraboloidal solar collection system determined by the method outlined herein is compared with that performance computed by utilizing the integrated energy entering a receiver calculated by the exact procedure of reference 4 in order to assess the effects of the approximations introduced in the analysis of this report. The results of applying the two methods are presented and compared in figure 8. The curves illustrate the overall collection efficiency of a paraboloidal collection system as a function of receiver aperture diameter for the misorientation range of 0 to 30 minutes. The collector is assumed to have a normal distribution of surface error with a standard deviation of 6 minutes. The two receiver operating temperatures considered are 2200° and 4000° R. The lower temperature represents the receiver operating temperature of currently designed solar turbodynamic power systems, such as the solar Brayton system, whereas the higher temperature is representative of advanced power system concepts, such as the solar thermionic system.

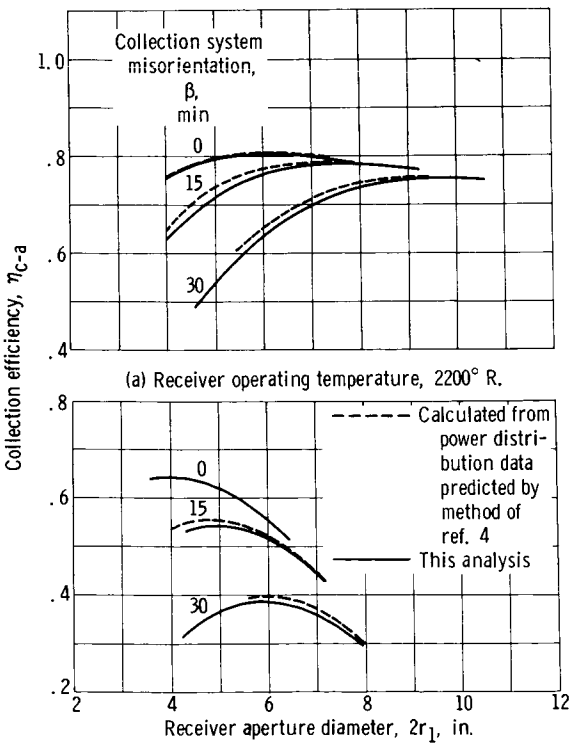

Figure 8. - Comparison of collection efficiency predicted by present analysis with that obtained by data of reference 4. Paraboloidal collector diameter, 30 feet; paraboloidal collector rim angle, 55°; collector standard deviation of surface error, 6 minutes; obstruction factor, 0.94; reflectivity, 0.90; receiver cavity, blackbody; receiver aperture closed during shadow portion of orbit.

It can be observed from figure 8 that, for perfect system orientation, there is little difference in the collection efficiency predicted by the two methods of calculation. For a misoriented collection system, the method of calculation presented herein predicts a slightly lower efficiency over the lower values of receiver aperture sizes. This is consistent with the conservative approximations employed to simplify the calculation of the amount of energy entering the receiver in a misoriented collection system.

In figure 8(a), the maximum collection efficiencies predicted by the two methods

differ by a quantity of less than 0.01 for the range of misorientation from 0 to 30 minutes at a receiver operating temperature of 2200° R. This difference, as shown in figure (8b), is less than 0.015 when the receiver operating temperature is as high as 4000° R.

Lewis Research Center,
National Aeronautics and Space Administration,
Cleveland, Ohio, August 2, 1966,
120-33-05-02-22.

APPENDIX A

SYMBOLS

A_c	projected area of paraboloidal collector
A_{ra}	area of receiver aperture
a	semimajor axis of ellipse in focal plane
b	semiminor axis of ellipse in focal plane
d	distance between center of image and focus
E	energy
E_{ce}	total energy in any circular element about center of image in focal plane
E_F	energy that enters receiver from each zone of focal plane when collection system is misoriented
E_T	total energy in region of focal plane
E_θ	energy intercepted by circular ring segment of paraboloid
F	focus of paraboloid
f	focal length of paraboloidal collector
H	effective emissivity of receiver to thermal radiation
K	solar constant measuring intensity of solar radiation in vicinity of collector, $Btu/(hr)(ft^2)$
k	distance between center of ellipse and center of reflected image of Sun in focal plane
P	probability that particular collector surface error ϵ exists
P_c	cumulative probability of all collector surface errors less than given value
R	radius of collector
r	radius of circular zone in focal plane surrounding center of image, ft
r_c	radial distance of collector element from optic axis, ft
r_1	radius of receiver aperture, in.
T	receiver operating temperature, ^oR
x	coordinate of intersection of circular zone in focal plane with receiver aperture
x_1, x_2	coordinates of intersection of circular zone in focal plane with that of ellipse
α	subtended half-angle of Sun at collector
α_S	effective absorptivity of receiver to solar radiation
β	angular misorientation of collection system, min

ϵ angular deviation of normal to surface of actual paraboloidal collector from ideal normal, measured in optic plane

ϵ_{av} average value of error

η_B obstruction efficiency of collection system

η_c concentration efficiency

η_{c-a} collection efficiency of system that measures net energy available to conversion system

η_E concentration efficiency measuring the integrated energy entering receiver as fraction of energy reflected from collector

η_R reflective efficiency or reflectivity

η_{rad} radiation efficiency that measures radiation losses from receiver

θ angular location of point on paraboloid from optic axis as measured from focus, deg

$\frac{\theta_o}{\theta_S}$ ratio of time receiver aperture is open to orbit Sun time

θ_{rim} angular location of rim of paraboloid, deg

ρ distance from focus to point on paraboloid

σ Stefan Boltzman constant, 1712×10^{-12} Btu/(hr)(ft^2)(^{o}R)

φ angle subtended by portion of circular element in focal plane common to given ellipse

φ_t defined by eq. (6)

$\varphi_{1,2}$ defined by fig. 4

ψ angle subtended by portion of circular zone in focal plane common to receiver aperture

APPENDIX B

DETERMINATION OF QUANTITY OF ENERGY INTERCEPTED BY RING ELEMENT OF COLLECTOR

The quantity of energy that is intercepted by a ring element of the collector is determined as follows (see fig. 2 for a description of the paraboloidal collector and its associated terminology).

A ring element of the collector at the average radius r_c with a projected width dr_c is assumed. The projected area of this segment of the collector is

$$A_c = 2\pi r_c \, dr_c \tag{B1}$$

and the energy being intercepted by this segment is

$$E = K2\pi r_c \, dr_c \tag{B2}$$

where K is the solar constant in the vicinity of the collector. The element has the polar coordinate θ and a width $d\theta$. The radius r_c of the element in terms of θ is

$$r_c = \rho \sin \theta \tag{B3}$$

$$dr_c = \rho \cos \theta \, d\theta + \sin \theta \, d\rho \tag{B4}$$

The distance ρ, between the focus and the element is provided by

$$\rho = \frac{2f}{1 + \cos \theta} \tag{B5}$$

where f is the focal length of the paraboloid, and

$$d\rho = -\frac{2f(-\sin \theta \, d\theta)}{(1 + \cos \theta)^2} = \frac{\rho \sin \theta \, d\theta}{(1 + \cos \theta)} \tag{B6}$$

Substituting equation (B6) into equation (B4) yields

$$dr_c = \rho \cos\theta \, d\theta + \frac{\sin\theta \, \rho \sin\theta \, d\theta}{(1 + \cos\theta)}$$

$$= \rho[\cos\theta + (1 - \cos\theta)] \, d\theta \qquad \text{(B7)}$$

$$= \rho \, d\theta$$

Substituting for $r_c \, dr_c$ in equation (B2) in terms of θ gives

$$E_\theta = K2\pi\rho \sin\theta\rho \, d\theta$$

$$= 2\pi k\rho^2 \sin\theta \, d\theta \qquad \text{(B8)}$$

which is the total energy being intercepted by any segment of the collector.

APPENDIX C

SAMPLE CALCULATION

The following example demonstrates the application of the results of the included analyses to predicting the general performance as well as the maximum collection efficiency of a power system that employs a paraboloidal collection system.

Determine the collection efficiency of a power system operating in a near-Earth orbit, which utilizes a collection system that consists of a 30-foot-diameter paraboloidal collector of 55° rim angle with a cavity receiver under a misorientation condition of 15 minutes. It is assumed that 6 percent of the incident solar energy is obstructed by the power equipment, that the collector surface reflectivity is 0.9, and that the receiver cavity behaves as a blackbody with an operating temperature of 2200° R. The receiver aperture is allowed to be shuttered during the dark phase of the orbit; that is, $\theta_o/\theta_s = 1$. It is assumed that the surface errors in the collector exhibit a normal distribution with a standard deviation of 6 minutes. This specification stipulates that at least 99 percent of the collector surface has an angular error value less than 15 minutes.

The normal distribution function is a continuous function with errors ranging from zero to infinity. This function is divided into various small bands of errors, the size of which is shown in table I, and the average error of each band ϵ_{av} is utilized to represent

TABLE I. - PROBABILITY VALUES OF VARIOUS COLLECTOR SURFACE ERRORS IN NORMAL DISTRIBUTION

[Standard deviation of surface error, 6 min.]

Error band	Average error, ϵ_{av}	Probability of error band,[a] P	Cummulative probability,[b] P_c
0 to 0.5	0.25	0.0664	0.0664
0.5 to 1.5	1.0	.1310	.1974
1.5 to 2.5	2.0	.1260	.3234
2.5 to 3.5	3.0	.1166	.4400
3.5 to 4.5	4.0	.1068	.5468
4.5 to 5.5	5.0	.0954	.6422
5.5 to 6.5	6.0	.0776	.7198
6.5 to 8.5	7.5	.1230	.8428
8.5 to 11.5	10.0	.1018	.9446
11.5 to 16.5	14.0	.0494	.9940

[a]Fraction of collector area with error in this band.

[b]Fraction of collector area with errors not exceeding error in this band.

that interval. This average error is assigned the total probability for the band, which prescribes the portion of the collector within that error range. The cumulative probability of each error is also included in table I to indicate the fraction of the collector area with an error value equal to or less than the given error magnitude.

In order to obtain the fraction of energy entering a given receiver aperture when the collector has a normal distribution of surface error, the fraction of energy entering the receiver (fig. 6(g)) for each of the errors associated with the distribution is multiplied by its probability (table I), and the products are added.

Repeating this procedure for several aperture sizes establishes the entering energy profile as a function of receiver aperture diameter. These data are presented in table II, and the respective curve is plotted in figure 9, which provides the value of η_E described in equation (18) for computing the collection efficiency.

The values of η_E are substituted into equation (18) to calculate the values of η_c, η_{rad}, and η_{c-a} as a function of the receiver aperture diameter $2r_1$. These values are presented in table III and are plotted in figure 10.

The tradeoff between η_c and η_{rad} optimizes when the receiver aperture diameter is 8 inches, as shown in figure 10, and the corresponding maximum collection efficiency is 78.5 percent.

TABLE II. - PERCENTAGE OF AVAILABLE ENERGY ENTERING RECEIVER OF VARIOUS APERTURE DIAMETERS FOR PARABOLOIDAL CONCENTRATOR WITH NORMAL DISTRIBUTION OF SURFACE ERROR

Average error, ϵ_{av}, min	Probability, P	Ratio of receiver to collector radius, r_1/R					
		0.01	0.015	0.020	0.025	0.030	0.035
		Fraction of available energy entering receiver, η_E					
0.25	0.0664	0.0580	0.0653	0.0664	0.0664	0.0664	0.0664
1.0	.1310	.1125	.1275	.1310	.1310	.1310	.1310
2.0	.1260	.1060	.1235	.1260	.1260	.1260	.1260
3.0	.1166	.0927	.1125	.1166	.1166	.1166	.1166
4.0	.1068	.0795	.1012	.1065	.1068	.1068	.1068
5.0	.0954	.0667	.0885	.0943	.0954	.0954	.0954
6.0	.0776	.0500	.0698	.0760	.0776	.0776	.0776
7.5	.1230	.0682	.1045	.1185	.1225	.1230	.1230
10.0	.1018	.0423	.0764	.0940	.1005	.1018	.1018
14.0	.0494	.0115	.0272	.0398	.0465	.0488	.0494
Total							
-----	------	0.6874	0.8964	0.9691	0.9893	0.9934	0.994

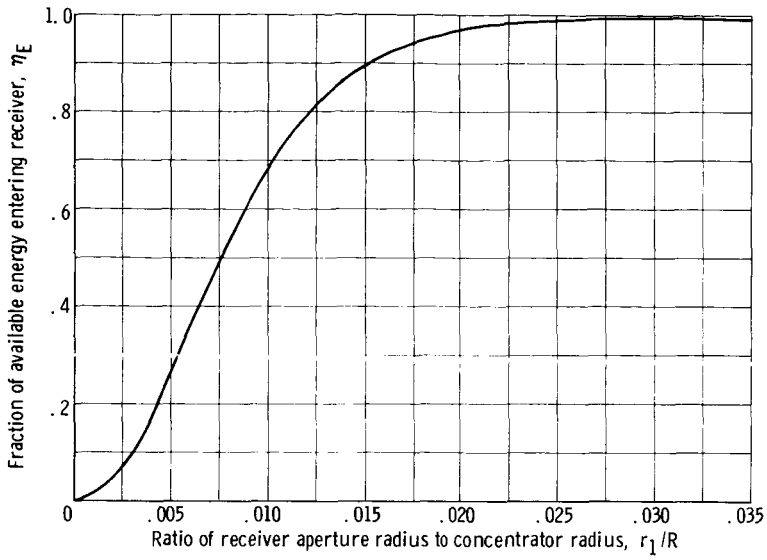

Figure 9. - Energy captured by receiver for paraboloidal collector with a normal distribution of surface error. Paraboloidal collector rim angle, 55°; collector standard deviation of surface error, 6 minutes; collection system misorientation, 15 minutes.

TABLE III. - EFFICIENCY OF PARABOLOIDAL COLLECTION SYSTEM AS FUNCTION OF RECEIVER APERTURE RADIUS

Collection efficiency, η_{c-a}	Ratio of receiver to collector radius, $\frac{r_1}{R}$	Receiver radius, r_1, in.	Fraction of available energy entering receiver, η_E	Concentration efficiency, $\eta_B\eta_R\eta_E\alpha_S$	Radiation losses, $\frac{\epsilon\sigma A_{ra}T^4}{\pi R^2 K}$
0.572	0.010	1.8	0.6874	0.582	0.01
.737	.015	2.7	.8964	.757	.02
.7815	.020	3.6	.9691	.818	.0365
.7785	.025	4.5	.9893	.835	.0565
.7565	.030	5.4	.9934	.838	.0815
.724	.035	6.3	.994	.839	.1150

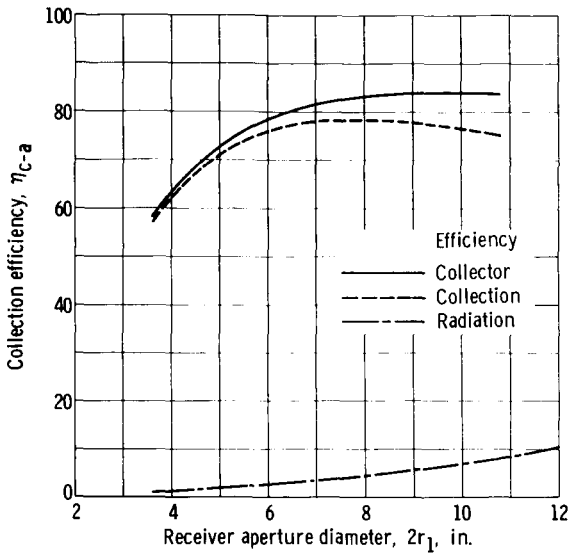

Figure 10. - Collection efficiency as function of receiver aperture size. Paraboloidal collector diameter, 30 feet; paraboloidal collector rim angle, 55°; obstruction factor, 0.94; reflectivity, 0.90; receiver operating temperature, 2200° R; collector standard deviation of surface error, 6 minutes; receiver cavity, blackbody; receiver aperture closed during shadow portion of orbit; collection system misorientation, 15 minutes.

REFERENCES

1. Hukuo, Nobuhei; and Mii, Hisao: Design Problems of a Solar Furnace. Solar Energy, vol. 1, no. 2-3, 1957, pp. 108-114.

2. McClelland, D. H.; and Stephens, C. W.: Energy Conversion Systems Handbook. Vol. II: Solar-Thermal Energy Sources. Rep. No. 390, vol. 2 (WADD TR 60-699, vol. 2, DDC No. AD-256973), Electro-Optical Systems, Inc., Sept. 1960.

3. Silvern, David H.: An Analysis of Mirror Accuracy Requirements for Solar Power Plants. Paper No. 1179-60, ARS, May 1960.

4. Schrenk, G. L.: Theoretical Analysis of Solar Reflectors. Rep. No. EDR 3193, Allison Division, General Motors Corp., July 1, 1963.

"The aeronautical and space activities of the United States shall be conducted so as to contribute . . . to the expansion of human knowledge of phenomena in the atmosphere and space. The Administration shall provide for the widest practicable and appropriate dissemination of information concerning its activities and the results thereof."

—NATIONAL AERONAUTICS AND SPACE ACT OF 1958

NASA SCIENTIFIC AND TECHNICAL PUBLICATIONS

TECHNICAL REPORTS: Scientific and technical information considered important, complete, and a lasting contribution to existing knowledge.

TECHNICAL NOTES: Information less broad in scope but nevertheless of importance as a contribution to existing knowledge.

TECHNICAL MEMORANDUMS: Information receiving limited distribution because of preliminary data, security classification, or other reasons.

CONTRACTOR REPORTS: Technical information generated in connection with a NASA contract or grant and released under NASA auspices.

TECHNICAL TRANSLATIONS: Information published in a foreign language considered to merit NASA distribution in English.

TECHNICAL REPRINTS: Information derived from NASA activities and initially published in the form of journal articles.

SPECIAL PUBLICATIONS: Information derived from or of value to NASA activities but not necessarily reporting the results of individual NASA-programmed scientific efforts. Publications include conference proceedings, monographs, data compilations, handbooks, sourcebooks, and special bibliographies.

Details on the availability of these publications may be obtained from:

SCIENTIFIC AND TECHNICAL INFORMATION DIVISION

NATIONAL AERONAUTICS AND SPACE ADMINISTRATION

Washington, D.C. 20546